Babol Noshirvani University of Technology

Journal of Structural and Earthquake Engineering

JOURNAL OF STRUCTURAL AND EARTHQUAKE ENGINEERING

Research Paper

Behavior of Bolted Steel Moment Frame Connection with End-Plate Under Elevated Temperature

Alireza Goltabar [1], Maziyar Barzegar [2], Hossein Yousefpour[3]

[1] Associate Professor Civil Engineering, Babol Noshirvani University of Technology, Babol, Iran, E-mail address: ar-goltabar@nit.ac.ir,
[2] Ph.D. Candidate, Faculty of Civil Engineering, Babol Noshirvani University of Technology, Babol, Iran, E-mail address: barzegar.maziyar@gmail.com,
[3] Associate Professor, Civil Engineering, Babol Noshirvani University of Technology, Babol, Iran, E-mail address: hyousefpour@nit.ac.ir

Article information

Received: March 15 2025.
Revised: April 30 2025.
Accepted for publication: May 25 2025.
Corresponding author:
A. Goltabar (ar-goltabar@nit.ac.ir).

Abstract

Fire poses a major threat to structures worldwide, particularly to steel structures, due to the well-known deterioration of steel strength at elevated temperatures. Among structural components, connections play a crucial role in transferring forces between load-bearing members, and their failure during fire can compromise the entire structural system. Despite this critical role, the high-temperature behavior of connections under fire conditions has been relatively underexplored. This paper presents a comprehensive numerical study on the thermo-mechanical response of bolted end-plate moment connections in steel frames subjected to fire. Nonlinear three-dimensional finite element models were developed and validated against experimental data to examine connection failure modes, mid-span beam deflection, and axial forces under elevated temperatures. The validated models were then used to perform parametric analyses to investigate the effects of beam length and end-plate thickness on the connection performance. The findings reveal that longer beam spans lead to failure at lower temperatures, with axial forces peaking and diminishing more rapidly as the temperature increases. Additionally, thicker end plates reduce bolt tensile forces and shift the dominant failure mechanism from the connection region to the beam itself.

Keywords: Steel moment frame, Bolted connection with endplate, Fire, High temperature, Finite Element Method.

1. Introduction

Fire safety in structures is a critical issue that has attracted considerable attention from researchers and engineers worldwide, particularly regarding steel structures. During a fire, the loss of strength and stiffness in structural materials, especially steel, combined with the development of thermal forces and deformations, significantly compromises the load-bearing capacity, stiffness, and overall stability of the structure. Consequently, fire protection has traditionally been provided through the use of insulating systems such as spray-applied fire-resistive materials (SFRMs) and gypsum boards, among other protective systems.

Determining the required amount of insulation against fire is generally done through a prescriptive method based on codes and standards published by reputable organizations. Most of these methods use the concept of fire resistance rating, which indicates the time required for a member under standard fire test conditions to lose its structural adequacy, integrity, and insulation. The required fire resistance rating depends on the building's occupancy, area, and height, the presence or absence of automatic sprinklers, the type of materials (combustible or non-combustible), access for firefighting, distance from adjacent buildings, etc.

Despite the widespread use of prescriptive methods, several limitations remain. For example, structural elements are typically assessed in isolation under fire exposure, while the thermal stresses and forces induced in the structure, as well as the interaction between members, are often neglected. To address these shortcomings, performance-based design approaches have been developed to simulate the actual structural behavior under fire, explicitly accounting for member interactions and force redistribution. Among the various structural components, connections play a particularly critical role in capturing these interactions.

Connections play a critical role in maintaining the overall stability of steel structures by ensuring efficient load transfer between structural elements. Beam-end connections in particular are subjected to substantial rotational demands. Under fire conditions, connection components experience a significant loss of strength and stiffness. Moreover, thermal expansion restraint generates large axial forces in both beams and connections [1-4].

Bolted connections are widely employed in steel structures to provide either fixed or pinned end conditions. Among these, endplate connections are one of the most commonly used options in steel buildings in Iran for Resistance against bending moment. To fully exploit the capacity of these moment connections while satisfying fire design requirements, it is essential to gain a comprehensive understanding of the force and deformation demands on endplate moment connections under fire conditions and to evaluate their resistance and deformation capacity at elevated temperatures. This need is further underscored by the experimental findings of Wang et al. [4], who demonstrated the susceptibility of these connections to large axial forces and bending demands induced by fire.

The necessity of investigating the behavior of connections under fire conditions has been demonstrated in numerous experimental and numerical studies. One of the most notable experimental programs was carried out by the Building Research Establishment (BRE) in Cardington, UK, where a series of full-scale fire tests were performed on an eight-story steel-framed building. The findings revealed that conventional design approaches for steel frames, which are primarily based on the behavior of individual members, fail to accurately capture the realistic local behavior and the overall structural response of steel frames exposed to fire [24].

Wang [5–8], through a series of parametric studies, demonstrated that maintaining connection performance during significant beam bending deformations at elevated temperatures allows the beam to sustain fire exposure for considerably longer durations. In a separate investigation, Memari et al. [25,26] analyzed the behavior of a single-span steel moment frame with Reduced Beam Section (RBS) connections under fire conditions. They employed the inter-story drift ratio as a key parameter to assess the overall stability of the analyzed frames under various fire scenarios. Their findings revealed that the progression of fire across floor levels does not substantially influence inter-story drift values, potentially explaining the lack of global structural collapse observed in single-compartment fire incidents in previous fire events [25,26]. Furthermore, Morovat et al. examined the influence of thermal creep on the response of shear tab connections. Their numerical model was validated against Wang's experimental results, followed by an extensive parametric investigation considering factors such as heating rate, cooling duration, initial cooling temperature, column size, beam geometry, and shear tab location, to evaluate the time-dependent behavior of frames during both the heating and cooling phases of fire [9,17–21].

Despite the aforementioned research efforts, substantial gaps persist in understanding the global response of endplate moment connections under fire exposure. For instance, the dominant failure mechanisms of these connections at elevated temperatures have not been thoroughly investigated. Moreover, the axial force demands induced by fire on beams and connections remain insufficiently quantified. Finally, current design practices often treat connections independently from the beam. While this approach may be adequate at ambient temperatures, it fails to capture the actual stiffness of connections at elevated temperatures, which critically affects the forces and deformations developed during fire conditions.

The objective of this study is to investigate the factors influencing the behavior of endplate connections under fire, with the aim of improving the design of these components to enhance beam performance at elevated temperatures. Finite element models of endplate connections at ambient and elevated temperatures are developed and validated against the experimental results reported by Wang et al. [4]. The validated models are then employed in a parametric study to identify the key parameters governing the behavior of endplate connections during the heating phase of a fire.

2. Numerical Modeling of End-Plate Moment Connections at Elevated Temperatures

2.1. Geometry of the Tested Connection Components (Flexural Connection)

To validate the proposed modeling approach, the experimental investigations conducted by Wang et al. [4] were adopted. This section outlines the geometry, material properties, and meshing of the structural components, as well as the analysis procedure involving applied loads, boundary conditions, and temperature distribution.

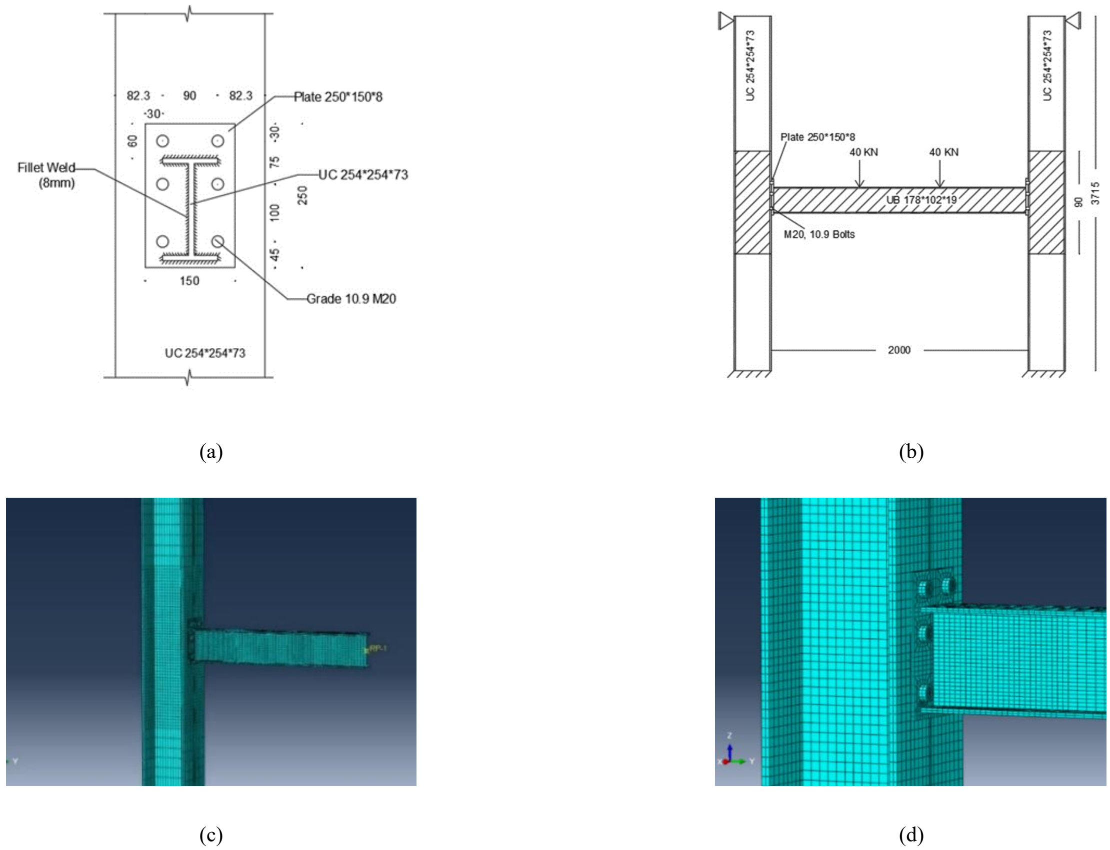

Fig. 1. Frame used in this study: (a) Components of the endplate moment connection [4]; (b) Schematic of the frame tested by Wang et al. [4]; (c) Half-frame finite element model in ABAQUS [16]; (d) Finite element model of the end-plate moment connection in ABAQUS [16].

2.2. Geometry of the Second Tested Connection Components (Shear Connection)

The second connection (shear connection) tested by Wang et al. [4] is shown in Figure 2. This sub-structure, similar to the moment connection in Figure 1, consists of a 2-meter-long I-section beam connected to two I-section columns, each 3715 mm long, through a shear plate measuring 150 × 130 mm with a thickness of 8 mm. The shear plate is welded to the column flange and bolted to the beam web using four M20 tension bolts with standard 20 mm diameter holes.

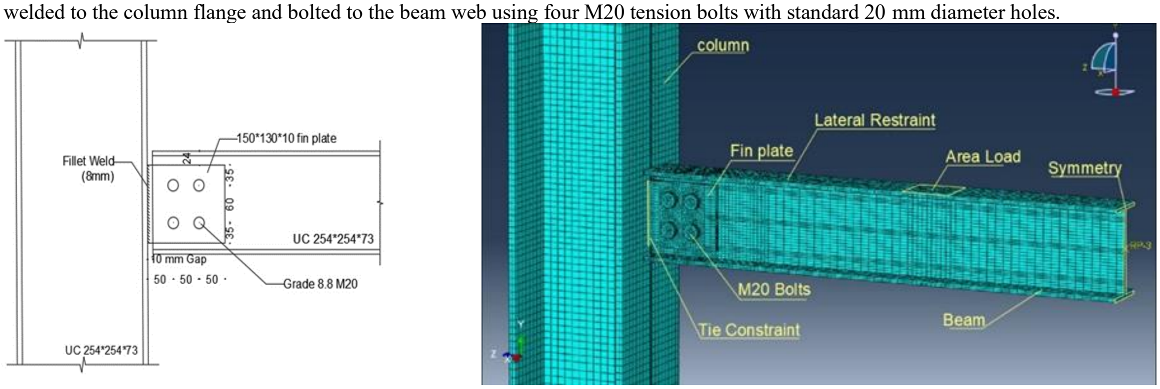

(a) (b)

Fig. 2. Frame investigated in this study: (a) Components of the shear connection [4]; (b) Model of half of the frame in Abaqus software [16].

2.3. Mechanical Properties

The specifications of different steel types used in the experimental specimens are presented in Table 1. The beam and end plate were fabricated from nominal S275 grade steel, while the columns were made of nominal S355 grade steel. Tensile tests, however, indicated that the actual mechanical properties of these components were slightly higher than the specified nominal values [4]. In the present study, an ideal bilinear (elastic–perfectly plastic) stress–strain relationship was adopted for all steel types. Bolt threads were not explicitly modeled; instead, a 25% reduction in bolt material strength was applied to account for potential thread stripping and yielding effects. Grade 10.9 bolts and nuts were used in the moment connection, whereas Grade 8.8 bolts were used for the shear connection [4,15]. Poisson's ratio was assumed to be 0.3 for all steel grades across all temperatures. The reduction in mechanical properties at elevated temperatures was incorporated in the numerical model based on Table 2, using retention factors from Li et al. [9] for structural steel and data from Hu et al. [14] for bolts.

Table 1. Mechanical properties of steel in the experiment by Wang et al. [4].

Steel components	Grade	Yield Stress (MPa)	Ultimate Stress (MPa)	Modulus of Elasticity (GPa)
Bolts and nuts	G10.9	900	1000	210
	G8.8	640	800	210
Column	S355	350	510	194
Beam	S275	250	450	233
Endplate	S275	350	500	167

Table 2. Steel strength retention factors in the numerical model.

Retention Factors for Frame Elements [9].			**Retention Factors for Bolts & Nuts** [14].		
Temperature (°C)	Modulus of Elasticity	Yield Stress	Temperature (°C)	Modulus of Elasticity	Yield Stress
20	1	1	20	1	1
200	0.909	0.928	100	0.9818	0.9818
300	0.843	0.769	200	0.95905	0.95905
400	0.83	0.688	300	0.9363	0.9363
500	0.771	0.611	400	0.6963	0.6963
600	0.492	0.427	500	0.4563	0.4563
700	0.274	0.21	600	0.2163	0.2163
800	0.176	0.084	700	0.16221	0.16221
900	0.163	0.069	800	0.10814	0.10814

2.4. Meshing Specifications and Contact Definitions in the Numerical Model

Figures 1c, 1d, and 2b show the overall views of the two three-dimensional numerical models developed using ABAQUS. All structural members were modeled with reduced-integration eight-node solid elements (C3D8R). A mesh sensitivity analysis was conducted based on preliminary studies. Accordingly, for the endplate moment connection, beam element sizes ranged from 10 to 17 mm, with a finer mesh (10 mm) applied in the plastic hinge regions at both beam ends and at the location of the concentrated load. For the columns, considering only global buckling, mesh sizes of 16 mm in the transverse direction and 32 mm in the longitudinal direction were used. At the connection regions and heat-exposed areas, a uniform mesh of 16 mm was applied in both directions. A finer mesh was adopted in the endplate, particularly around the bolt holes. Along the plate thickness, 4 elements were used in the endplate, while 2 elements were used in the remaining areas.

For the shear connection, the mesh sizes for the beam, column, and shear plate were selected similarly to those of the moment connection. Bolt heads were idealized as cylindrical elements. A finer mesh was applied in the connection region, where failure is anticipated, to accurately capture stress distribution. The mapped meshing technique was employed around bolt holes to prevent stress concentration. Surface-to-surface contact with the finite sliding formulation was used in Abaqus. Tangential behavior was defined with a friction coefficient of 0.25, and normal behavior was modeled as hard contact, allowing separation, sliding, and rotation at the contact surfaces [20]. A tie constraint was applied to simulate the weld between the beam and the endplate.

2.5. Loading and Boundary Conditions

Considering the geometric and loading symmetry, only half of the steel frame was modeled in the Abaqus environment, and a symmetry boundary condition was applied at the mid-span of the beam to reduce computational time. Two distinct loading steps were defined in the numerical analysis:

Step 1: Application of bolt pretension by imposing an equivalent compressive force along the bolt axis to simulate the initial tensile stress, replicating actual installation conditions.

Step 2: Application of a concentrated vertical load of 40 kN on the top surface of the beam, corresponding to half of the plastic moment capacity of the beam section at ambient temperature, based on the experimental results by Wang et al. [4]. To prevent stress concentration, the load was distributed over a rectangular area measuring 150 × 101.2 mm.

After applying the mechanical load, the system temperature was gradually increased while maintaining the mechanical load constant. The boundary conditions were defined by the experimental setup as follows:

- The bottom support of the column was fixed, restraining all degrees of freedom.
- The top support of the column was free in the vertical direction and restrained in the horizontal direction.
- The top flange of the beam was restrained horizontally to simulate the lateral restraint effect provided by the reinforced concrete slab (which was not modeled).It is noteworthy that in Wang et al.'s experiment [4], this restraint was applied using a steel truss, as the composite interaction between the beam and slab was not considered, and the slab functioned solely as thermal insulation.
- During the bolt pretensioning step, bolts were restrained against displacement to ensure effective contact between the nut face, bolt head, and steel member.

2.6. Thermal Loading

Similar to the experimental studies by Wang et al. [4], the ISO 834 curve was used to impose elevated temperatures. In the experimental setup, the furnace dimensions were 900 × 1600 × 3000 mm; therefore, only a 900 mm segment of the column was positioned inside the furnace and exposed to high temperatures in the heat transfer analysis. Furthermore, the top flange of the beam was covered with a ceramic fiber insulation layer to replicate the thermal effect of a concrete slab. Notably, the concrete slab was not modeled due to the absence of interaction between the beam and the slab.

In the heat transfer analysis, the Specific Heat Capacity (Cp), Thermal Conductivity (K), and Convection Coefficient (hc) were derived from Eurocode 3 [10]. To apply radiation effects, the Stefan-Boltzmann constant ($\sigma = 5.67 \times 10^{-8}$ W/m²K⁴) was used, and for the emissivity coefficient (ε), recommendations from the Swedish Steel Institute were adopted, with $\varepsilon_{res} = 0.7$ for elements exposed to fire and $\varepsilon_{res} = 0.3$ for elements not exposed to fire.

Heat transfer from hot gases during a fire occurs through convection and radiation at the exposed surfaces of the structural member, followed by conduction through the member thickness. A three-dimensional transient heat transfer analysis was performed in Abaqus using the following formulation:

$$\frac{\partial T}{\partial t} = \frac{k}{\rho c}\left(\frac{\partial^2 T}{\partial x^2} + \frac{\partial^2 T}{\partial y^2} + \frac{\partial^2 T}{\partial z^2)}\right) \tag{1}$$

Where:

- T is the temperature
- t is time
- k is the thermal conductivity
- ρ is the density
- c is the specific heat capacity
- x, y, z are the spatial coordinates

2.7. Numerical Analysis Procedure

In the numerical simulation of the steel frame, transient thermal analysis was performed to account for the time-dependent variation of connection temperatures observed in the experiment [4]. Initially, the transient heat transfer analysis was carried out in Abaqus using the ISO 834 standard fire curve, and the resulting temperature distribution was subsequently applied as the thermal load in the structural mechanical analysis.

For the mechanical analysis of both moment and shear connections, the Static-General solver is used. In the models where creep effects are not considered, the static analysis is conducted using the Newton–Raphson algorithm. To address numerical convergence issues, a numerical stabilization scheme is applied using artificial damping. To maintain solution accuracy, the ratio of viscous dissipation energy (ALLSD) to total internal strain energy (ALLIE) is set to approximately 10^{-5}. Additionally, to ensure the reliability of the analysis, the summation of reaction forces is compared with the total applied loads to confirm equilibrium [20].

3. Comparison of Finite Element Predictions with Experimental Results

For the studied structures, including a beam with axial restraint and an endplate moment connection, as well as a beam with a shear connection, the predictions of the finite element models are compared with experimental results in Figures 3, 4, and 6. The comparisons demonstrate good agreement, confirming the accuracy and reliability of the finite element modeling approach.

As shown in Figure 3a, axial force develops in the steel beam due to restrained thermal expansion. At the initial stages of heating, the beam exhibits a linear increase in axial force and a slight rise in mid-span deflection, as the material properties remain largely unaffected at low temperatures. As the temperature rises further, the reduction in material strength and stiffness leads to a non-linear increase in both axial force and deflection.

From the results presented in Figures 3a and 3b, it is evident that although the axial force in the beam increases significantly during heating, it drops to zero at a temperature of 754 °C, while the mid-span deflection reaches 82 mm. At 767 °C, the beam deflection increases to 101 mm, which, according to BS 5950, is considered indicative of structural failure (as the deflection reaches one-twentieth of the span) [4]. Figure 4 indicates that the ductility of the endplate moment connection is primarily governed by endplate deformation. Figure 5 illustrates the beam deformation at the end of the analysis, corresponding to a temperature of 818 °C.

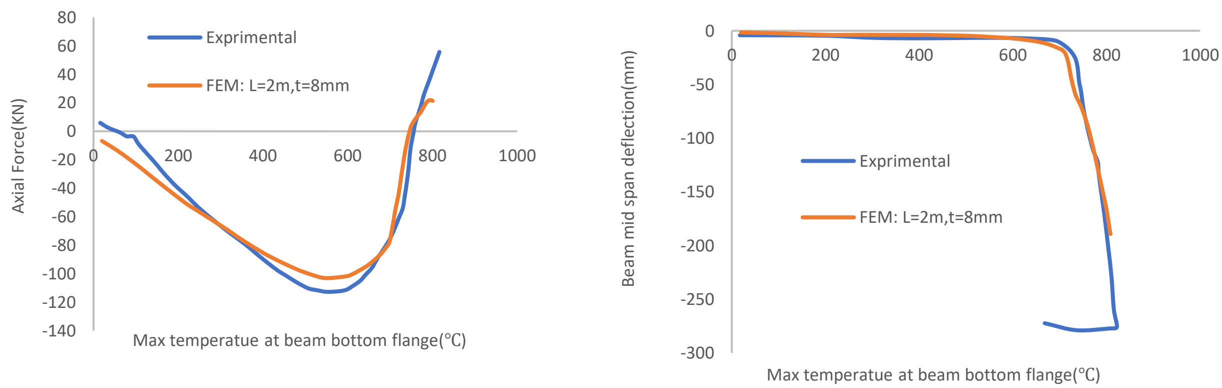

(a) (b)

Fig. 3. Comparison of deformation between the present finite element model and the reference experimental results [4]: (a) axial force in the beam; (b) mid-span deflection of the beam.

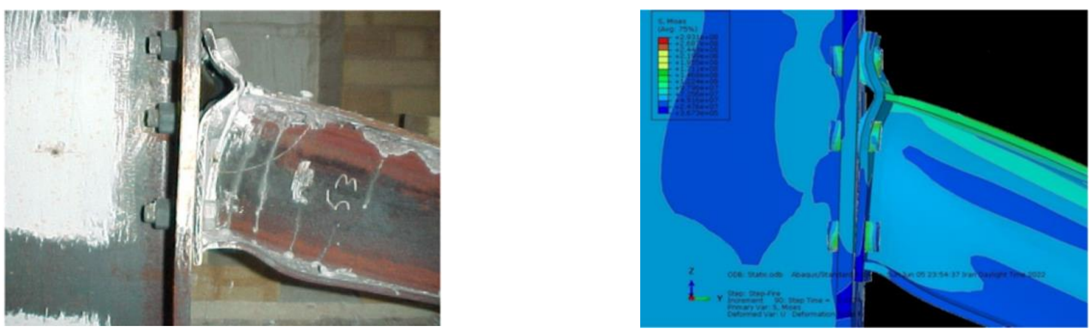

Fig. 4. Comparison between finite element model results and experimental results [4, 16].

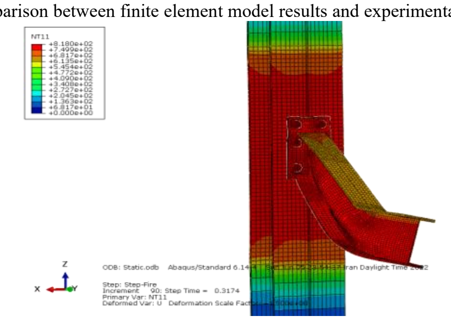

Fig. 5. Deformation of the finite element model at high temperature.

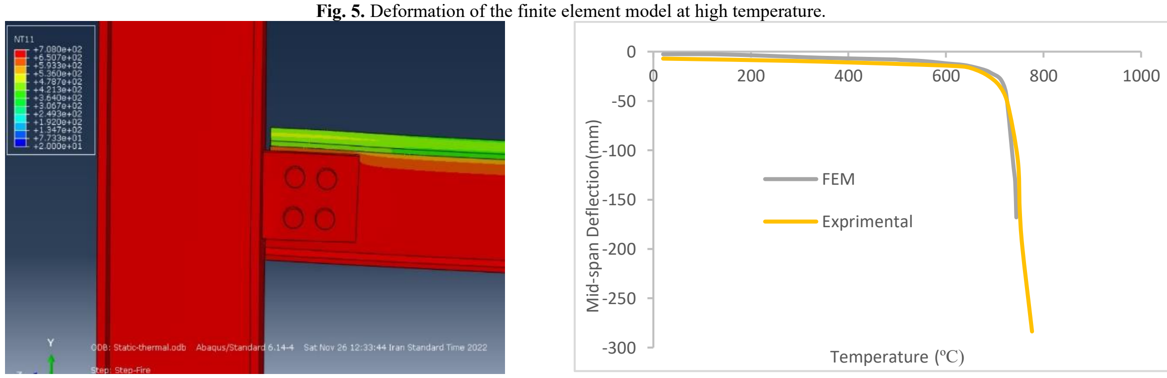

(a) (b)

Fig. 6. (a) Deformed shape of the finite element model at 708 °C ; (b) Comparison of beam deformation between the present finite element model and Wang's experimental model [4].

Figure 6a shows that the beam deflection remains negligible up to approximately 200 °C. Beyond this temperature, the deflection gradually increases due to the restrained thermal expansion of the beam, showing good agreement with the experimental results reported by Wang et al. [4].

4. Parametric Studies

To identify the key parameters influencing the behavior of endplate moment connections at elevated temperatures, a series of three-dimensional finite element models of the connection were developed and analyzed under high-temperature conditions. In this parametric study, the ISO 834 standard fire curve was employed as the temperature–time history. The composite concrete slab was not modeled; however, its effects in terms of heat transfer and lateral restraint were considered. Additionally, the influence of thermal creep in steel on the connection performance was not included in the analysis.

The steel frame was modeled in accordance with the validated study. The frame consists of a beam with an overall depth of 178 mm, a flange width of 102 mm, and a flange thickness of 19 mm, connected to two columns with an overall depth of 254.6 mm, a flange width of 254.6 mm, and a flange thickness of 14.2 mm via an endplate measuring 150 × 250 mm. The variable parameters considered in this parametric study were the beam lengths (2, 4, and 6 m) and the endplate thickness (8, 12, and 16 mm).

The endplate, following the experimental configuration by Wang et al. [4], was assumed to be bolted to the column flange using six M20 tension bolts with 20 mm diameter holes and welded to the beam. To facilitate numerical modeling and prevent convergence issues, the bolt threads were not explicitly modeled; instead, the ultimate strength of the bolts was taken as 0.75 of the nominal material strength [15]. The material properties of the bolts and steel components at both ambient and elevated temperatures were consistent with those used in the validation study. For each M20 bolt, a pre-tensioning force of 103.67 kN was applied, reflecting the 25% reduction in strength due to simplified thread modeling. The pre-tensioning was applied prior to beam loading to ensure stable contact and proper tightening of the connection. Additionally, a supplementary analysis was conducted with a minimal pre-tensioning force, applied only to close the connection, to investigate the influence of bolt pre-tensioning on the tensile and axial response of the connection.

Concentrated loads of 40 kN were applied to the beam at locations corresponding to 0.3 times the beam length from each end. The columns were free to move vertically but restrained in the horizontal direction. As the primary focus of this study is to examine the effects of connection details on the structural response at elevated temperatures, no vertical loads were applied to the columns, and out-of-plane displacements and torsional deformations were prevented. Additionally, the top flange of the beam was laterally restrained to simulate the stabilizing effect of the concrete slab as lateral bracing.

5. Effect of Key Parameters

Following validation of the finite element model, a parametric study was carried out to examine the influence of key parameters on the behavior of the endplate moment connection under fire conditions. The parameters considered were the beam span and the endplate thickness. The baseline model for this investigation was the validated model described in Section 2.

5.1. Effect of Beam Length

Three different beam spans were considered: 2 m (baseline), 4 m, and 6 m. The resulting axial force and mid-span deflection as functions of temperature are presented in Figures 7 and 8, respectively.

As shown in Figures 7a and 7b, the maximum axial compressive force occurs at 548 °C, 245 °C, and 344 °C for beam spans of 2 m, 4 m, and 6 m, respectively. The highest peak compressive forces are observed for the 2 m and 4 m beams. Moreover, at temperatures exceeding 400 °C, the maximum compressive and tensile forces in the 4 m and 6 m beams show only minor differences. Figure 7a indicates that increasing the beam span results in failure due to deformation at lower temperatures. Specifically, for the 2 m span beam, failure occurs at 767 °C with a mid-span deflection of 101 mm, according to BS 5950 criteria. For the 4 m beam, failure is observed at 663 °C with a deflection of 207 mm, representing a 205% increase relative to the 2 m beam. Similarly, the 6 m beam fails at 649 °C with a deflection of 304 mm, corresponding to a 300% increase compared to the 2 m span beam.

This behavior is attributed to a shift in the location of the governing failure mechanism. For the 2 m beam, failure occurs primarily in the endplate. In the 4 m beam, the mechanism involves both the beam element and the endplate. For the 6 m beam, failure occurs predominantly within the beam itself, leading to larger deflections. As observed in Figure 7, with increasing beam span, the axial force reaches its peak and subsequently reduces to zero at lower temperatures.

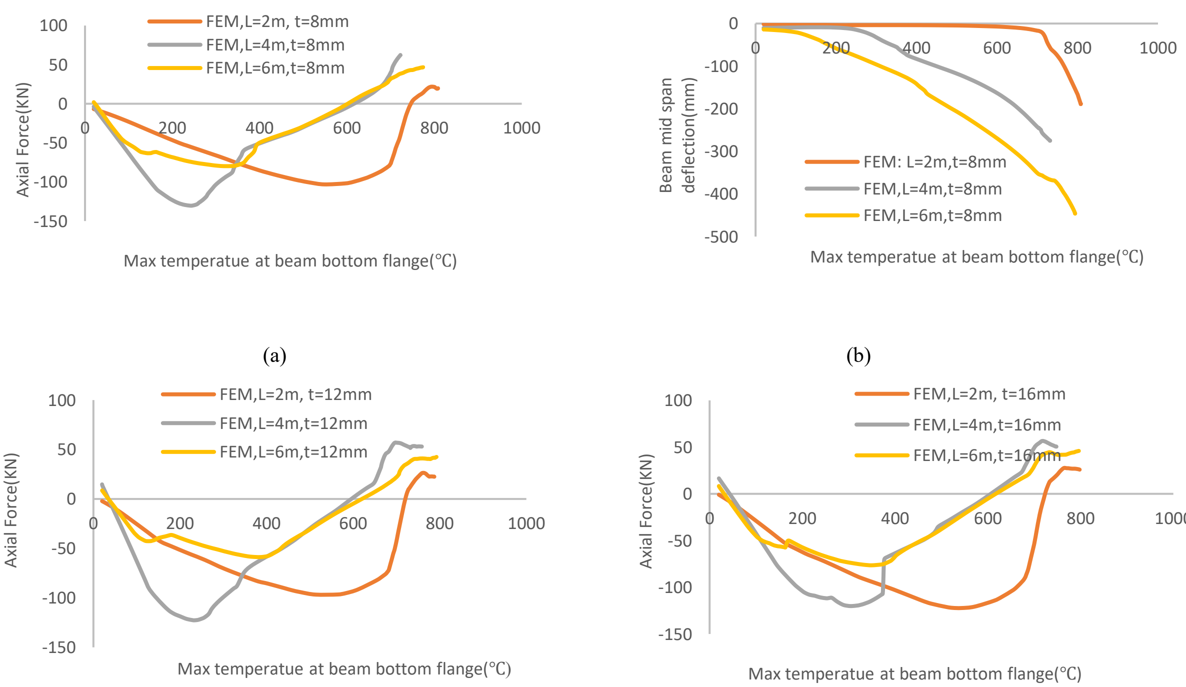

(a) (b)

(c) (d)

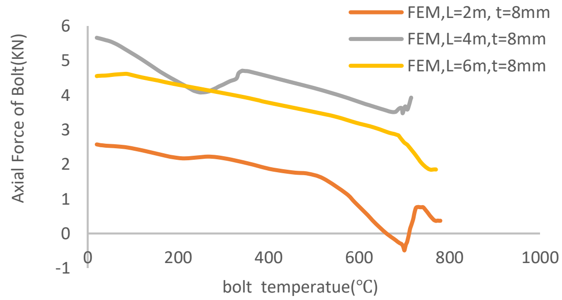

(m)

Fig. 7. Comparison between numerical model results for different beam lengths (L) and endplate thicknesses (t): (a) Beam axial force with t=8mm; (b) Mid-span beam deflection; (c) Beam axial force with t=12mm; (d) Beam axial force with t=16mm; (m) Bolt axial force

According to Figure 7m, due to the applied heat, the elastic modulus and yield stress of the bolts are reduced according to Table 2. In the pre-yield range, this leads to a reduction in bolt force at a relatively constant axial bolt deformation.

The variations in beam axial force under different endplate thicknesses are presented in Figure 8. As shown, increasing the endplate thickness affects the connection's response under elevated temperatures; however, this effect is less pronounced compared to the influence of beam span. Figure 7 demonstrates that changing the beam length, while keeping the endplate thickness constant, leads to a noticeable variation in the beam axial force and the temperature at which the axial force drops to zero. In contrast, Figure 8 shows that varying the endplate thickness for a constant beam span does not significantly alter the temperature at which the axial force reaches zero. For all three endplate thicknesses considered, the axial force approaches zero within a similar temperature range. Additionally, the differences in axial force among the three plate thicknesses are relatively minor at a given temperature. Similar to the effect of beam span, as the beam length increases, the axial force attains its peak at lower temperatures and subsequently decreases to zero earlier.

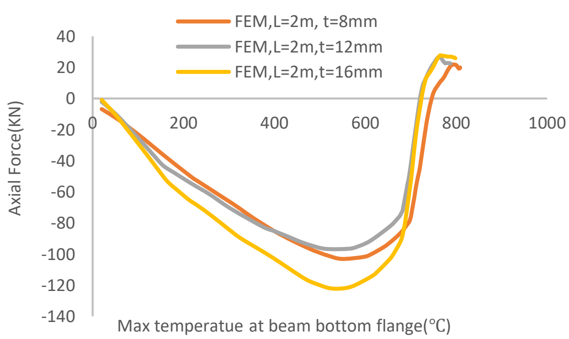

(a)

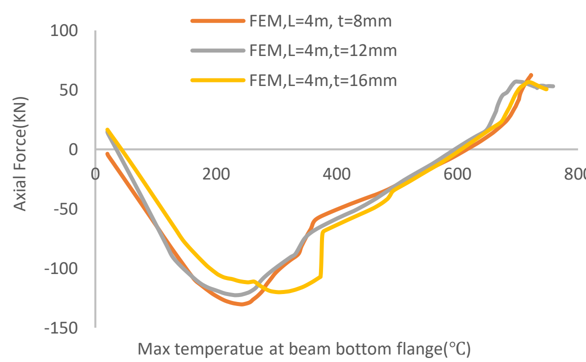

(b)

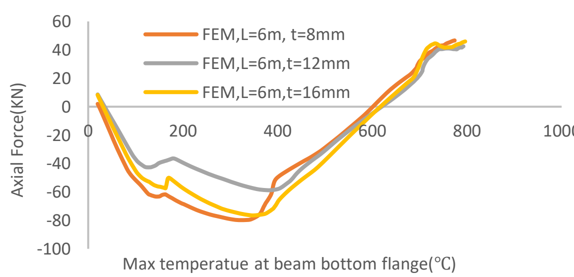

(c)

Fig. 8. Comparison between numerical model results for different beam lengths (L) and endplate thicknesses (t):(a) Beam axial force with L=2m; (b) Beam axial force with L=4m; (c) Beam axial force with L=6m.

Figure 9 illustrates the effect of beam length, at a constant endplate thickness, on endplate deformation. As shown, increasing the beam length from 2 m to 4 m results in a significant reduction in plate deformation, from 6.3 mm for the 2 m span beam to 4.18 mm for the 4 m span beam, representing approximately a 66.34% decrease. With further increases in beam length, the failure mechanism shifts away from the connection and into the beam, leading to smaller changes in endplate deformation. For the 6 m span beam, the deformation decreases to 1.97 mm, corresponding to an approximately 47.8% reduction compared to the 4 m span beam.

This reduction in endplate deformation at elevated temperatures with increasing beam span is attributed to the relocation of the governing failure mechanism. As illustrated in Figure 11, when the beam span increases, the failure mechanism moves away from the endplate, resulting in lower tensile forces being transferred to the endplate through the bolts and the beam.

During the phase of restrained thermal expansion induced by fire, the investigated structure experiences high compressive forces, resulting in a substantial axial force in the beam during the heating stage. This axial force increases with temperature until it reaches its maximum, as illustrated in Figures 7 and 8. Subsequently, the mid-span deflection of the beam accelerates, as shown in Figure 7a, due to the reduction in stiffness and strength caused by elevated temperatures. At peak temperatures, failure occurs in the beam due to web buckling and the formation of plastic hinges. The thermal bending deflection of the beam can be calculated using the following equation:

$$\delta_{th} = \frac{\alpha_T \cdot \Delta T \cdot L^2}{h} \tag{2}$$

Where α_T is the thermal expansion coefficient [10], ΔT is the temperature difference between the upper and lower flanges of the beam, L is the beam length, and h is the beam depth, equal to 177.8 millimeters (mm).

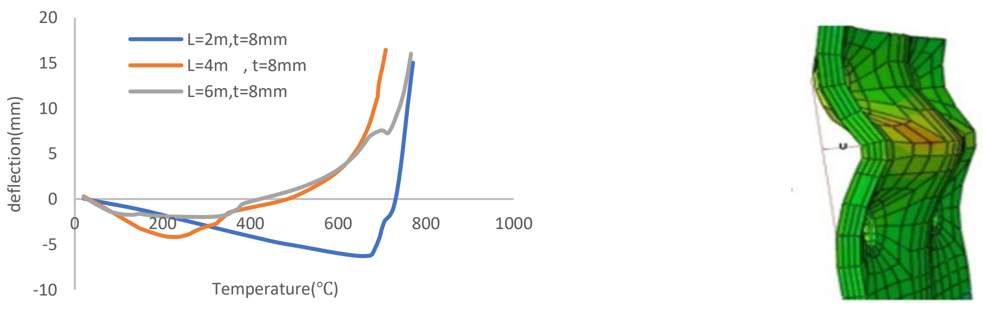

(a) (b)

Fig. 9. (a) Deformation diagram of the endplate; (b) Deformed finite element model of the end bending plate.

5.2. Effect of End-Plate Thickness

Three different endplate thicknesses were considered: 8 mm (baseline), 12 mm, and 16 mm. The influence of endplate thickness on the beam's axial force and mid-span deflection is presented in Figures 9 and 10.

Increasing the endplate thickness is expected to enhance its load-bearing capacity while reducing the tensile forces in the bolts. As shown in Figure 10, increasing the endplate thickness from 8 mm to 12 mm leads to a substantial decrease in bolt tensile forces, whereas further increases beyond 12 mm result in only marginal reductions.

Figures 7 and 10 indicate that increasing the beam span from 2 m to 4 m significantly amplifies the sensitivity of bolt tensile forces to the endplate thickness. For longer beam spans, the tensile forces in the bolts decrease due to a shift in the load transfer mechanism from the endplate to the beam, as illustrated in Figure 9.

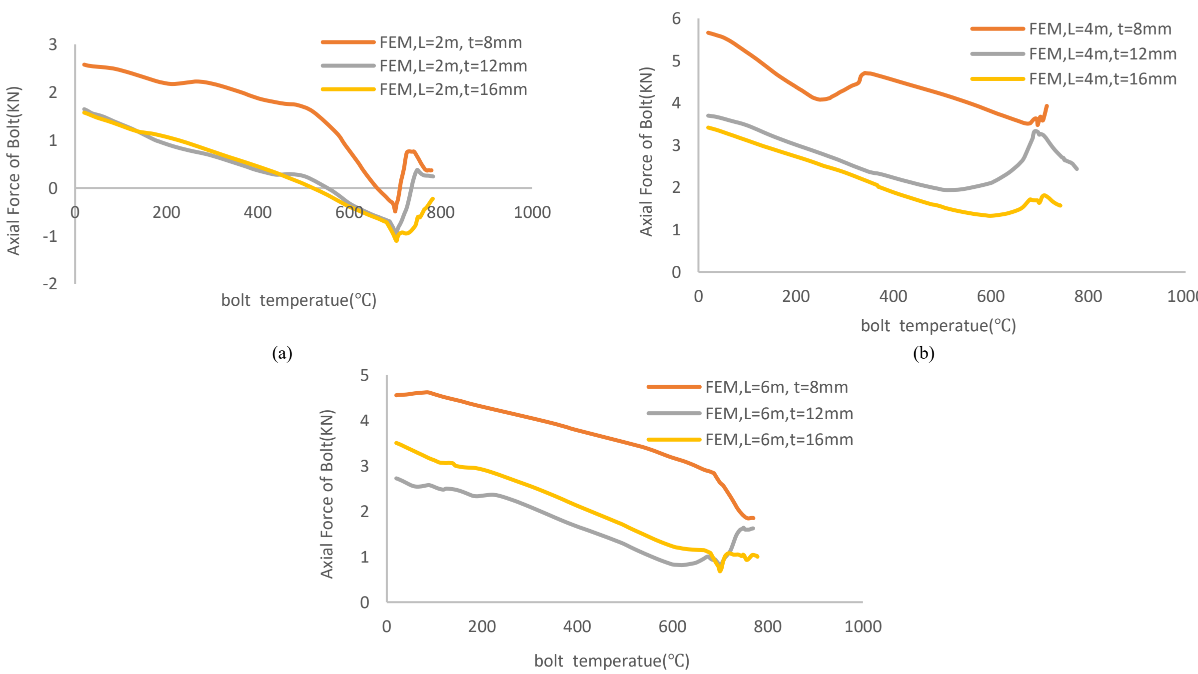

(c)

Fig. 10. Axial forces versus bolt temperature for various beam length: (a) 2 meters, (b) 4 meters, and (c) 6 meters.

Figure 11 illustrates the connection behavior of the beam for three different endplate thicknesses. As observed from Figures 11 and 7a, increasing the beam span shifts the governing failure mechanism away from the endplate toward the beam, resulting in larger beam deflections (Figure 7a) and reduced axial forces in the bolts (Figure 7m). Furthermore, Figure 7a indicates that for longer beams, a plastic hinge forms at lower temperatures, further amplifying the beam deflection. Figure 9 shows that, for beams with a constant endplate thickness, the axial force in the bolts decreases as the span length increases, reaching its maximum at lower temperatures. At the same time, the deformation of the endplate associated with the potential failure mechanism is reduced.

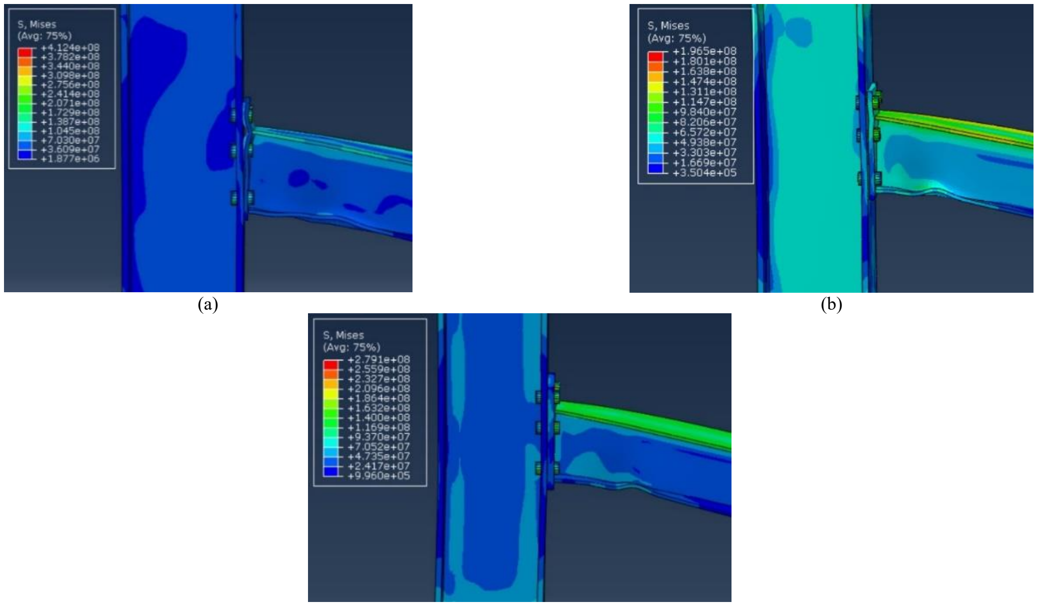

(a) (b)

(c)

Fig. 11. Comparison of failure mechanisms for a 6 m beam connection with varying endplate thicknesses(t):(a): Endplate thickness: t = 8 mm; (b): Endplate thickness: t = 12 mm; (c): Endplate thickness: t = 16 mm.

5.3. Effect of Bolt Pre-tensioning Force

Figure 12 shows that applying a minimal preload to the bolts results in considerable joint deformation and pronounced bolt elongation. In this case, the preload was applied solely to ensure closure of the connection. As a consequence, substantial elongation occurs in the bolts, particularly in the upper row, emphasizing the critical influence of the bolt pre-tension magnitude on the structural behavior of the connection. Under this condition, the axial tensile force in the bolts is equivalent to the externally applied load.

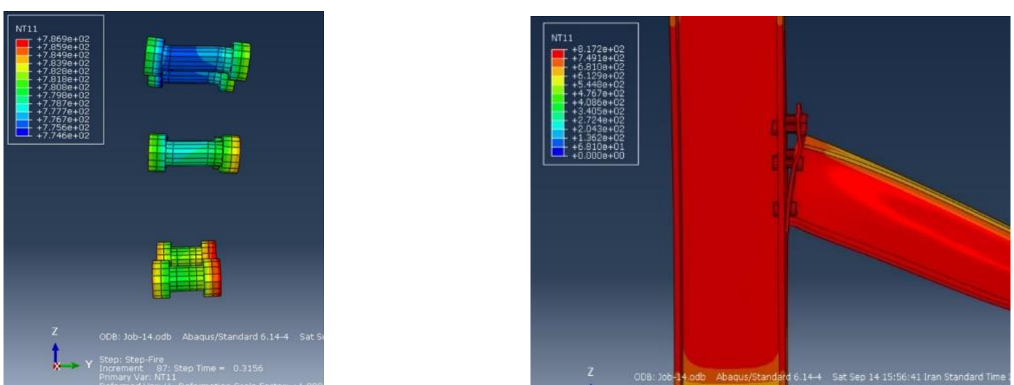

(a) (b)

Fig. 12. (a) Bolt elongation under minimal pre-tensioning force; (b) Joint deformation under minimal pre-tensioning force.

6. Conclusions

This study investigated the behavior of bolted steel moment frame connections with end-plates under elevated temperatures induced by fire using finite element analysis. The numerical models were validated against experimental data, and a parametric study was subsequently conducted. Based on the results, the following conclusions can be drawn:

1. The developed 3D finite element models accurately predict axial force development, mid-span deflection, and failure modes of end-plate moment connections under fire conditions, showing good agreement with experimental results.
2. Significant axial compressive forces develop in beams with restrained ends due to thermal expansion during fire. These forces increase with temperature initially but then decrease as steel properties degrade.
3. Increasing the beam span length leads to lower maximum axial forces but significantly larger mid-span deflections. Failure (large deflection) occurs at lower temperatures for longer beams.
4. Increasing the end-plate thickness enhances the rotational stiffness of the connection, leading to reduced mid-span beam deflection and lower tensile forces in the bolts.

5. Increasing the endplate thickness can shift the governing failure mode at high temperatures from bolt fracture and end plate yielding towards yielding and local buckling in the beam adjacent to the connection. This suggests that strengthening the endplate can improve the connection's fire performance but may make the beam the weaker link.
6. The findings highlight the importance of considering the connection behavior and its interaction with the beam in the fire safety design of steel structures. Performance-based approaches incorporating realistic connection modeling are crucial for accurate assessment.

Author Contributions

The manuscript was written through the contribution of all authors. All authors discussed the results, reviewed, and approved the final version of the manuscript.

Conflict of Interest

The author(s) declared no potential conflicts of interest concerning the research, authorship, and publication of this article.

Funding

The author(s) received no financial support for the research, authorship, and publication of this article.

Data Availability Statements

The datasets generated and/or analyzed during the current study are available from the corresponding author on reasonable request.

References

[1] G. Hu, Behavior of beam shear connections in steel buildings subject to fire (Ph.D. Dissertation), The University of Texas at Austin, USA, 2011.

[2] T.C.H. Liu, M.K. Fahad, J.M. Davies, Experimental investigation of behavior of axially restrained steel beams in fire, J.Constr.Steel Res.58(9)(2002) 1211–1230.

[3] C.G. Bailey, I.W. Burgess, R.J. Plank, Analyses of the effects of cooling and fire spread onsteel-framed buildings, Fire Saf. J. 26 (4)(1996)273–293.

[4] Wang, Y. C., X. H. Dai, and C. G. Bailey. "An experimental study of relative structural fire behaviour and robustness of different types of steel joint in restrained steel frames." Journal of Constructional Steel Research 67.7 (2011): 1149-1163.

[5] Wang YC, Yin YZ. Feasibility of utilising catenary action to eliminate fire protection to steel beams. In: Shen ZY, Li GQ, Chan SL, editors. Fourth International Conference on Advances in Steel Structures. Oxford: Elsevier Science Ltd; 2005.

[6] Yin YZ, Wang YC. A numerical study of large deflection behaviour of restrained steel beams at elevated temperatures. J Constr Steel Res 2004;60: 1029-47.

[7] Yin YZ, Wang YC. Analysis of catenary action in steel beams using a simplified hand calculation method, part 1: theory and validation for uniform temperature distribution. J Constr Steel Res 2005;61: 183-211.

[8] Yin YZ, Wang YC. Analysis of catenary action in steel beams using a simplified hand calculation method, part 2: validation for non-uniform temperature distribution. J Constr Steel Res 2005;61: 213-34.

[9] Lee J, Morovat MA, Hu G, Engelhardt MD, Taleff EM (2013) Experimental investigation of mechanical properties of ASTM A992 steel at elevated temperatures. Eng J 50:249–272.

[10] CEN, Eurocode 3: Design of Steel Structures Part 1.8: Design of Joints and Building Frames ENV 1993-1-8:2005, Brussels, Belgium, 2005.

[11] Lawson, R. M., and G. M. Newman. Fire resistant design of steel structures: a handbook to BS 5950: Part 8. SCI, 1990.

[12] NIST. Final Report on the Collapse of World Trade Cente r Building 7, Report NIST NCSTAR 1A, National Institute of Standards and Technology, Gaithersburg, MD, 2008.

[13] Chen, L., and Y. C. Wang. "Methods of improving survivability of steel beam/column connections in fire." Journal of Constructional Steel Research 79 (2012): 127-139.

[14]. Hu, Y., et al. "Comparative study of the behaviour of BS 4190 and BS EN ISO 4014 bolts in fire." Proceedings of 3rd international conference on steel and composite structures. 2007

[15] Al Haddad, Hadi O., Elie G. Hantouche, and Karim K. Al Khatib. "Numerical studies on the creep behavior of shear endplate connection assemblies under transient heating." Fire Technology 55 (2019): 2341-2367.

[16] DS-Simulia, Abaqus Version 6.14 Documentation. Providence, RI, 2014.

[17] Hajjar, Mohammad A., and Elie G. Hantouche. "Predicting the Demand of Shear Tab Connections with Composite Beams in Fire." International Journal of Steel Structures (2020): 1-16.

[18] Morovat, Mohammed Ali, et al. "Creep properties of ASTM A992 steel at elevated temperatures." Advanced Materials Research. Vol. 446. Trans Tech Publications Ltd, 2012.

[19] Cowan, Maria, and Kapil Khandelwal. "Modeling of high temperature creep in ASTM A992 structural steels." Engineering structures 80 (2014): 426-434.

[20] Al Khatib, Karim, Elie Hantouche, and Mohammed Ali Morovat. "Thermal creep of shear tab connection assemblies under transient-state temperatures of fire." Journal of Structural Fire Engineering (2019).

[21] Hantouche EG, Sleiman SA (2017) Axial restraint forces in shear endplates of steel frames due to fire. J Constr Steel Res 128:528–541.

[22] Hu Y, Davidson B, Burgess I, Plank R (2008) Experimental study on flexible endplate connections in fire. In: Proceedings of 5th European conference on steel structures, Graz, Austria, pp 1007–1012.

[23] Kodur VR, Dwaikat MM (2010) Effect of high temperature creep on the fire response of restrained steel beams. Mater Struct 43(10):1327–1341.

[24] Ziemian, R.D., ed. 2010. Guide to Stability Design Criteria for Metal Structures. 6th Edition. New York: John Wiley & Sons, Inc.

[25] Memari, Mehrdad, and Hussam Mahmoud. "Performance of steel moment resisting frames with RBS connections under fire loading." Engineering structures 75 (2014): 126-138.

[26] Memari, Mehrdad, and Hussam Mahmoud. "Multi-resolution analysis of the SAC steel frames with RBS connections under fire." Fire Safety Journal 98 (2018): 90-108.

[27] Mahmoud, Hussam, et al. "Response of steel reduced beam section connections exposed to fire." Journal of structural engineering 142.1 (2016): 04015076.

[28] Rahnavard, Rohola, and Robert J. Thomas. "Numerical evaluation of the effects of fire on steel connections; Part 1: Simulation techniques." Case studies in thermal engineering 12 (2018): 445-453.

[29] Rahnavard, Rohola, and Robert J. Thomas. "Numerical evaluation of the effects of fire on steel connections; Part 2: Model results." Case Studies in Thermal Engineering 13 (2019): 100361.

[30] Lien, K. H., et al. "Nonlinear behavior of steel structures considering the cooling phase of a fire." Journal of Constructional Steel Research 65.8-9 (2009): 1776-1786.

[31] Elsawaf, S., and Y. C. Wang. "Behaviour of restrained structural subassemblies of steel beam to CFT column in fire during cooling stage." Engineering structures 46 (2013): 471-492.

[32] Selamet, Serdar, and Maria E. Garlock. "Modified connection details for single plate steel connections under fire." Structures Congress 2009: Don't Mess

with Structural Engineers: Expanding Our Role. 2009.

[33] Wang, Peijun, Guoqiang Li, and Shixiong Guo. "Effects of the cooling phase of a fire on steel structures." Fire safety journal 43.6 (2008): 451-458.

[34] Elsawaf, S., and Y. C. Wang. "Methods of improving the survival temperature in fire of steel beam connected to CFT column using reverse channel connection." Engineering structures 34 (2012): 132-146.

[35] Elsawaf, S., and Y. C. Wang. "Behaviour of restrained structural subassemblies of steel beam to CFT column in fire during cooling stage." Engineering structures 46 (2013): 471-492.

ORCID iD

Alireza Goltabar —

Maziar Barzegar —

Hossein Yousefpour —

Use this format to cite this article:

Goltabar, A., Barzegar, M., Yousefpour, H., "Behavior of Bolted Steel Moment Frame Connection with End-Plate Under Elevated Temperature," *Journal of Structural and Earthquake Engineering*, 1(2), pp. 51–62, 2025.